

# Coherent amplification of ultrashort pulses in activated crystals

O. P. Varnavskii, A. N. Kirkin, A. M. Leontovich, R. F. Malikov, A. M. Mozharovskii, and E. D. Trifonov

*P. N. Lebedev Physics Institute, Academy of Sciences of the USSR, Moscow*

(Submitted 18 August 1983)

Zh. Eksp. Teor. Fiz. **86**, 1227–1239 (April 1984)

A theoretical and experimental study is reported of the coherent amplification of picosecond pulses in Nd:YAG and ruby at 100 K. The basic features of coherent amplification that distinguish it from noncoherent amplification have been observed. They are: the onset of sign-changing oscillations of the field envelope on the trailing edge of the amplified pulse, the absence of restrictions on the pulse length due to the gain linewidth, and the appearance of a doublet structure in the emission spectrum. Good agreement between experimental and theoretical results was achieved.

## §1. INTRODUCTION

Coherent interaction is usually defined as the interaction between electromagnetic radiation and a resonance medium for which the pulse length  $\tau_p$  is less than the time  $T_2$  of phase (transverse) relaxation of the medium. Relaxation processes do not then modify the phase of the atomic wave functions during the interaction time, and a resonant macroscopic polarization is produced in the medium. This leads to a number of specific effects, such as nutation, free induction, photon echo, self-induced transparency, superradiance, and so on.<sup>1</sup> The study of coherent effects in the optical range began relatively recently, and has been largely confined to absorbing media. So far as amplifying media are concerned, most published papers have been theoretical (see, for example, Refs. 2–4). Experimental studies were reported only in a few publications,<sup>5–7</sup> and were concerned with the amplification of nanosecond pulses and gases. Systematic studies of coherent amplification were not performed and, therefore, many of the interesting effects predicted by theory have not as yet been observed. This is probably due to the fact that, until quite recently, the coherent amplification conditions were usually not realized to any significant extent in the active media commonly employed. However, the advent of subpicosecond lasers<sup>8</sup> and the use of new active media in ultrashort pulse generators (UPG) has made the problem of coherent amplification very topical from the practical point of view as well.

In this paper, we report a theoretical and experimental study of the generation and amplification of ultrashort pulses in Nd:YAG and ruby at a temperature of about 100 K, when the pulse length is less than the transverse relaxation time of the medium. Preliminary results were published in Refs. 9 and 10. The first experimental results on coherent interaction in the picosecond range were reported in our earlier papers.<sup>11,12</sup> Self-induced transparency was observed in the absence of the pump in ruby.<sup>13</sup>

## §2. THEORY OF COHERENT AMPLIFICATION

Resonant coherent amplification in the semiclassical approximation for the nondegenerate two-level system is usually described by the Maxwell-Bloch equations for the

electric field  $E(r, t)$  and the atomic density matrix  $\|\rho_{ik}(r, t)\|$  (Refs. 1, 14, and 15)

$$\begin{aligned} \left( \Delta - \frac{n^2}{c^2} \frac{\partial^2}{\partial t^2} - \kappa \frac{\partial}{\partial t} \right) E &= \frac{4\pi}{c^2} \frac{\partial^2}{\partial t^2} P, \\ \dot{\rho}_{bb} &= -\gamma_{bb}\rho_{bb} + i \frac{\mu}{\hbar} E (\rho_{ab} - \rho_{ba}), \\ \dot{\rho}_{aa} &= -\gamma_{aa}\rho_{aa} - i \frac{\mu}{\hbar} E (\rho_{ab} - \rho_{ba}), \\ \dot{\rho}_{ba} &= -\gamma_{ba}\rho_{ba} + i \frac{\mu}{\hbar} E (\rho_{aa} - \rho_{bb}) - i(\omega_0 + \Delta)\rho_{ba}, \quad \rho_{ab} = \rho_{ba}^*, \end{aligned} \quad (1)$$

where  $P(r, t)$  is the polarization (dipole moment per unit volume of the medium), which can be expressed in terms of the density matrix

$$P(r, t) = N_0 \mu \int_{-\infty}^{\infty} d\Delta G(\Delta) \{ \rho_{ab}(r, t, \Delta) + \rho_{ba}(r, t, \Delta) \}, \quad (2)$$

$\mu$  is the matrix element of the transition dipole moment between levels  $a$  and  $b$ ,  $N_0$  is the initial inversion density in the medium (in the case of complete inversion,  $N_0$  is the number of atoms per unit volume),  $\omega_0$  is the pulse carrier frequency which coincides with the center of the inhomogeneously-broadened line,  $G(\Delta)$  is the inhomogeneous broadening profile,  $\gamma_{aa}, \gamma_{ab}, \gamma_{bb}$  are the relaxation constants,  $\Delta$  is the shift of the atomic transition frequency from  $\omega_0$ ,  $n$  is the refractive index,  $c$  is the velocity of light, and  $\kappa$  represents the volume radiation loss.

The solution for  $E$  and  $\rho_{ab}$  is usually sought in the form of plane transverse waves propagating in a particular direction:

$$\begin{aligned} E(x, t) &= \mathcal{E}^+(x, t) \exp [i(\omega_0 t - k_0 x)] \\ &+ \mathcal{E}^-(x, t) \exp [-i(\omega_0 t - k_0 x)], \\ \rho_{ba}(x, t, \Delta) &= R^-(x, t, \Delta) \exp [-i(\omega_0 t - k_0 x)], \\ \rho_{ab}(x, t, \Delta) &= R^+(x, t, \Delta) \exp [i(\omega_0 t - k_0 x)], \end{aligned} \quad (3)$$

where  $k_0 = n\omega_0/c$ ,  $\mathcal{E}^- = (\mathcal{E}^+)^*$ ,  $R^- = (R^+)^*$ .

In the approximation of slowly-varying amplitudes, (1) yields the so-called set of truncated equations which, in terms of dimensionless variables, have the form

$$\begin{aligned} \frac{\partial A^\pm}{\partial \xi} + \frac{\partial A^\pm}{\partial \tau} &= -\kappa A^\pm + \int_{-\infty}^{\infty} R^\pm(\xi, \tau, \Delta') g(\Delta') d\Delta', \\ \frac{\partial R^\pm}{\partial \tau} &= \left( \pm i\Delta' - \frac{1}{\tau_2} \right) R^\pm + 2A^\pm Z, \\ \frac{\partial Z}{\partial \tau} &= -(A^- R^+ + A^+ R^-), \end{aligned} \quad (4)$$

where  $A^\pm = n\mathcal{E}^\pm / \pm i(2\pi N_0 \hbar \omega_0)^{1/2}$  is the dimensionless field amplitude,  $\tau = t\Omega$ ,  $\xi = x\Omega/v$  are, respectively, the dimensionless time and position coordinate,  $\Omega = (\mu/n\hbar)(2\pi N_0 \hbar \omega_0)^{1/2}$ , is the population inversion normalized to a single atom, and  $v = c/n$ ,  $\tau_2 = T_2 \Omega = \Omega/\gamma_{ab} = \Omega/\gamma_{ba}$ ,  $\Delta' = \Delta/\Omega$ ,  $g(\Delta')d\Delta' = G(\Delta)d\Delta$ . It is assumed in (4) that  $\gamma_{aa} = \gamma_{bb} = 0$ , i.e., the longitudinal relaxation time is  $T_1 = \infty$ . The vector with components  $\text{Re } R^+$ ,  $\text{Im } R^+$ ,  $Z$  is called the Bloch vector. The frequency  $\Omega$  is equal to the Rabi frequency for the coherent field, whose energy density is  $W = |\mathcal{E}^\pm|^2/2\pi = N_0 \hbar \omega_0$ . The dimensionless field  $A$  is the ratio of the Rabi frequency of the radiation field to  $\Omega$ , i.e., the relative Rabi frequency. It will be seen later that this quantity can be appreciably greater than unity.

In the general case, for sufficiently large  $T_2$ , the McCall-Hahn area theorem

$$d\theta/dx = \alpha \sin \theta; \quad \theta(x) = \frac{\mu}{\hbar} \int_{-\infty}^{\infty} \text{Re } \mathcal{E}^+(x, t) dt, \quad (5)$$

is satisfied for both amplifying and absorbing media, where  $\theta(x)$  is the pulse area and  $\alpha$  is the unsaturated amplification coefficient at the line center ( $\alpha < 0$  for an absorbing medium). According to (5), the variation in the overall pulse area occurs until it becomes equal to  $\pi(2n - 1)$  for the amplifying medium and  $2\pi n$  for the absorbing medium.

The area theorem (5) is a general analytic result deduced from (4). However, it provides no information about the pulse shape of the variation in this shape during propagation. As regards exact solutions, these can be obtained only in special cases. For example, if we neglect volume losses ( $\kappa = 0$ ) and homogeneous broadening ( $T_2 = \infty$ ), the system has simple soliton solutions that were first obtained by studying self-induced transparency<sup>16</sup>

$$\text{Re } \mathcal{E}^+ = \frac{2\hbar}{\tau_p \mu} \text{sech} \left[ \left( t - \frac{x}{u} \right) / \tau_p \right], \quad (6)$$

where  $u$  is the pulse velocity which can be approximately described by the formula

$$n/c = 1/u + 1/2\alpha\tau_p. \quad (7)$$

The area of this pulse is  $2\pi$ .

For an absorbing medium, Eq. (6) determines the stationary  $2\pi$ -pulse. For the inverted medium, the  $2\pi$ -pulse is unstable. Its velocity differs from the phase velocity of light in the medium, and can be greater than this velocity. It is interesting that the sign of the velocity  $u$  may be different from that of the phase velocity of light. The excess over and above the velocity of light, and the reversal of the sign of the group velocity, are due to the amplification of the infinitely extended leading front of the pulse. The instability of  $2\pi$ -pulses in inverted media is a consequence of the instability of the initial and final states of the system. We note that it was

pointed out in the experimental Ref. 5 that there was a tendency for the propagation velocity of the pulse maximum to increase in comparison with the phase velocity of light.

When a sufficiently short pulse of initial area  $\theta_0$  passes through an inverted medium, the subsequent evolution of the field can be described by the self-similar solution of (4) (Refs. 17-19)

$$A = \frac{1}{2} \frac{\xi}{(T\xi)^{1/2}} \theta'(w), \quad (8)$$

where  $T = \tau - \xi$ ,  $w = 2(T\xi)^{1/2}$ . The polar angle of the Bloch vector, numerically equal to  $\theta$ , satisfies the equation

$$\frac{d^2\theta}{dw^2} + \frac{1}{w} \frac{d\theta}{dw} - \sin \theta = 0, \quad \theta(0) = \theta_0. \quad (9)$$

During its propagation, the pulse given by (8) contracts in proportion to the traversed path, and its intensity increases as the square of this path length. Such pulses are characterized by field oscillations due to optical nutation under the influence of the amplified pulse. Their spectra exhibit double structure due to the dynamic Stark effect.<sup>20</sup>

The self-similar solution is formally available for the  $\delta$ -shaped exciting pulse. Since the scale of the self-similar solution is determined by the quantity  $\tau_R = \Omega^{-2}c/2Ln$  ( $L$  is the length of the system), the length of the input pulse must be of the order of  $\tau_R$  or less. The self-similar solution will also arise when homogeneous and inhomogeneous broadening is taken into account, provided

$$T_2, T_2^* > \left| \ln \frac{\theta_0}{2\pi} \right|^2 \tau_R,$$

where  $T_2^*$  is the reciprocal inhomogeneous width. It was suggested in Refs. 19 and 21 that, for large amplifier lengths, the solution will tend asymptotically to the self-similar solution, and will be practically independent of the initial conditions. The degree of correspondence with the self-similar solution for finite lengths and real conditions of amplification in Nd:YAG and ruby will be illustrated below by a numerical solution of (4).

### §3. CALCULATION OF THE AMPLIFICATION OF ULTRASHORT PULSES IN Nd:YAG AND RUBY

We have carried out a theoretical study of the shape and spectrum of ultrashort pulses, amplified in Nd:YAG and ruby, using a numerical solution of (4). The calculation was performed for transitions between the components  $R_1 - Y_1$  of the  ${}^4F_{3/2} - {}^4I_{11/2}$  multiplets in Nd:YAG and for the line  $R_1$  in ruby at temperatures close to 100 K. It was assumed that the levels were nondegenerate. This is completely justified for Nd:YAG in which, for a twofold Kramers degeneracy of the working levels, the transition dipole moments are all equal. The situation is more complicated in the case of ruby. Nevertheless, it will be seen below that, even in this case, good agreement with experiment can be achieved.

The parameters that were varied in our calculation were  $T_2$ ,  $T_2^*$ ,  $\alpha L$  (amplification for a weak signal), and the input area of the pulse  $\theta_0$ . Spectroscopic data reported in Refs. 22-24 were used to determine the parameters of these transi-

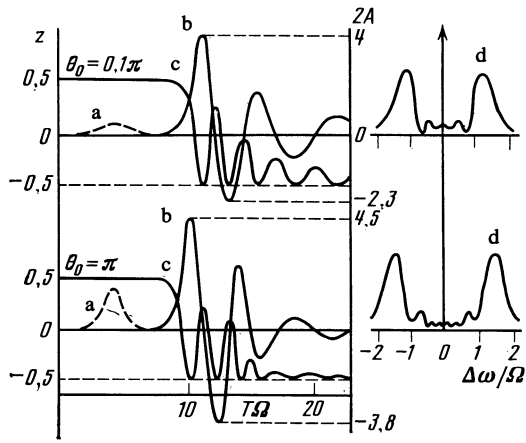


FIG. 1. Effect of the input-pulse area on the dynamics and spectrum of the pulse amplified by Nd:YAG crystal: a—input pulse, b—output pulse, c—population dynamics at the end of the specimen, d—spectrum of amplified pulse;  $T_2 = T_2^* = \infty$ ,  $L = 6$  cm,  $\alpha L = 5$ .

tions. The transition dipole moments in ruby and Nd:YAG were taken to be  $1.5 \times 10^{-20}$  and  $4 \times 10^{-20}$  esu, respectively. The characteristic time scale  $\Omega^{-1}$  was 50 and 40 ps for amplification in ruby and Nd:YAG, respectively, with initial amplification  $\alpha L = 6$  and  $\alpha L = 5$ . The input pulse was specified in the form of a hyperbolic secant. It was assumed that there was no phase modulation.

Figure 1 shows graphs illustrating the effect of  $\theta_0$  on the dynamics and spectrum of the amplified pulse in Nd:YAG in the absence of relaxation. Analysis of these results shows that the shape of pulses with  $\theta_0 < 2\pi$  varies so as to ensure that the area of the main pulse approaches  $2\pi$ . The damping of the residual-polarization pulse induced by the field shows itself in the shape of the oscillations after the main pulse. This part of the signal is qualitatively described by the self-similar solution of the Maxwell-Bloch set of equations, used in the theory of superradiance (Refs. 17, 25, 26). The area of the oscillations is  $-\pi$ , i.e., the total area under the amplified signal tends to  $\pi$ , in accordance with the area theorem. Since the area of the main pulse is  $2\pi$ , its energy grows more slowly than the energy of the signal as a whole. The latter grows faster (by a factor of two) than in the usual noncoherent amplification, when the final inversion in the medium is zero at best. The characteristic doublet structure analogous to the superradiance spectrum appears in the spectrum of the amplified signal. It may be looked upon as a manifestation of dynamic Stark broadening in the field of the pulse. The splitting of the spectrum and the frequency of the field oscillations are of the order of the Rabi frequency for the pulse field. As the oscillations become damped, their frequency will therefore fall. Inversion maxima correspond to the zeros of the field envelope. Inversion minima (all atoms in the lowest state) correspond to the extrema of the field or intensity maxima.

Variation of  $\theta_0$  between  $0.1\pi$  and  $2\pi$  produces a rise in the size of the output-signal maxima and to a reduction in the oscillation period. This is accompanied by only a slight change in the doublet structure of the spectrum. When  $\theta_0 \gg 2\pi$ , the input ultrashort pulse splits into two  $2\pi$ -pulses.

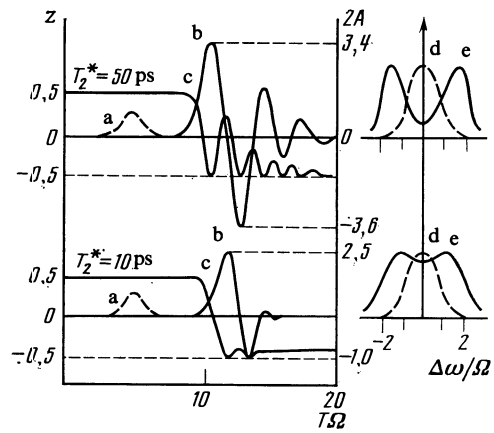


FIG. 2. Effect of inhomogeneous broadening on the dynamics and spectrum of the pulse amplified by Nd:YAG: a—input pulse, b—output pulse, c—population dynamics at exit from the specimen, d and e—spectra of input and output pulses;  $T_2 = \infty$ ,  $L = 6$  cm,  $\alpha L = 5$ ,  $\theta_0 = 0.5\pi$ .

The time structure of the field becomes complicated because of the superposition of the oscillations produced by each of the  $2\pi$ -pulses separately.

The above general features remain valid even when  $T_2$  and  $T_2^*$  are finite but sufficiently large. Their influence is illustrated by the graphs shown in Figs. 2 and 3. Transverse relaxation has little effect on the first peak of the output signal, but suppresses subsequent oscillations and the doublet structure of the spectrum. The presence of inhomogeneous broadening (finite  $T_2^*$ ) leads to the weakening of the oscillations, including a reduction in the height of the first peak. This is explained by a reduction in the effective number of atoms participating in the amplification process. An increase in the length of the amplifier produces a reduction in the width of the pulse of amplified radiation, and a corresponding rise in the height of the principal and secondary peaks.

We have calculated the intensity of the amplified pulse under conditions as close as possible to the experimental conditions. Figures 4 and 5 show the results for Nd:YAG and ruby for different values of  $T_2$ . We note that there is a substantial difference between the peak intensities for

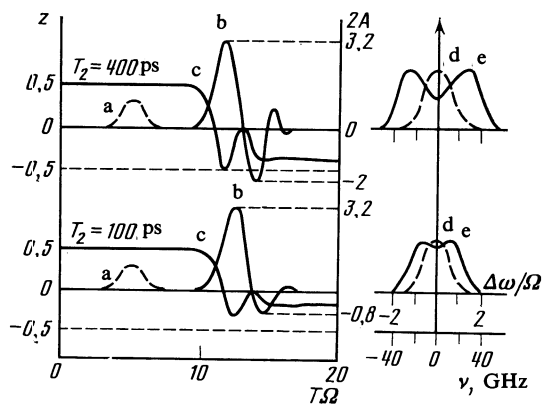


FIG. 3. Effect of transverse relaxation on the dynamics and spectrum of the pulse amplified in Nd:YAG: a—input pulse, b—output pulse, c—population dynamics at exit from the specimen, d and e—spectra of input and output pulses;  $T_2^* = 20$  ps,  $L = 6$  cm,  $\alpha L = 5$ ,  $\theta_0 = 0.5\pi$ .

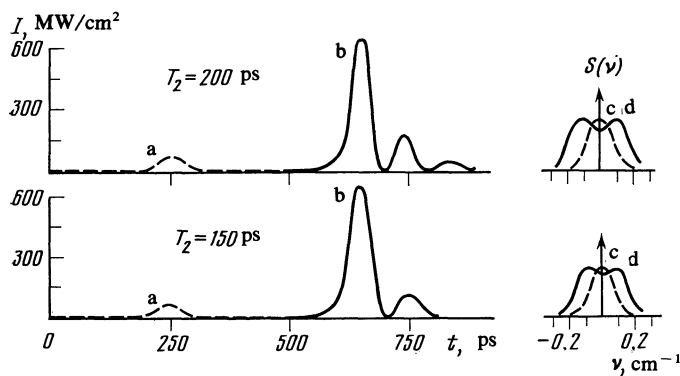


FIG. 4. Coherent amplification by Nd:YAG: a and b—input and output pulses, c and d—spectra of input and output pulses;  $L = 6$  cm,  $\alpha L = 5$ ,  $T_2^* = 20$  ps,  $\theta_0 = 0.5\pi$ .

Nd:YAG and ruby. This is due to the difference between the dipole moments of the working transitions. It is clear that a reduction in  $T_2$  is accompanied by the suppression of the intensity oscillations on the trailing edge of the pulse. This enables us to estimate  $T_2$  from time scans of the emission intensity.

#### §4. EXPERIMENT

The aim of our experiments was to observe the main features of coherent amplification that distinguish it from noncoherent amplification, namely, oscillations in the intensity of the emitted radiation on the trailing edge of the pulse. The alternation in the sign of the field envelope, the absence of basic limitations on the pulse length due to the width of the line associated with the amplifying transition, and the appearance of the doublet structure in the spectrum.

##### 1. Media under investigation

We have investigated the amplification of picosecond pulses in Nd:YAG and ruby at 100 K. These media are very convenient because, on the one hand, they are readily available and, on the other, they have different parameters of active transitions, so that it is interesting to compare the results obtained for them. The coherent nature of the interaction between picosecond pulses and ruby under these conditions was established in Ref. 13, where we investigated self-induced transparency. In addition to increased transmission, we recorded a substantial (by a factor of up to two) reduction in the velocity of the ultrashort pulses, which is characteristic for this effect.<sup>16</sup>

The quantities  $T_2$  and  $T_2^*$  can be estimated under our conditions from the spectroscopic data on the temperature dependence of linewidths corresponding to the  $R_1-Y_1$  (Nd:YAG) and  $R_1$  (ruby) transitions. Since the transitions in

which we are interested occur to ground or long-lived states, the line is essentially inhomogeneously broadened for  $T \rightarrow 0$ . Since the inhomogeneous linewidth is a slowly-varying function of temperature, and since we know the total linewidth at 100 K, we can estimate the contributions of homogeneous and inhomogeneous broadening, i.e.,  $T_2$  and  $T_2^*$ . Using the data reported in Refs. 22 and 23 for ruby and in Ref. 24 for Nd:YAG, we conclude that  $T_2$  lies in the range 100–150 ps for both media. Both in Nd:YAG and in ruby, the inhomogeneous linewidth was found to be  $\sim 1$  cm<sup>-1</sup>, which corresponds to  $T_2^* \sim 20$  ps.

The dimensions of the Nd:YAG rods were  $5 \times 60$  and  $8 \times 80$  mm, and the respective Nd concentrations were 1% and 0.6%. We also used ruby crystals of  $12 \times 120$  mm and Cr concentrations of about  $1.5 \times 10^{19}$  cm<sup>-2</sup>. The rods were cooled down to about 100 K by the stream of vapor from a dewar containing liquid nitrogen.<sup>27</sup> The inhomogeneity in the longitudinal temperature distribution did not exceed 2 K. The rods were pumped by pulsed IFP-800 (Nd:YAG) and IFP-2000 (ruby) sources. An electrooptic camera with a resolution of 20 ps was used to investigate the time parameters of the ultrashort pulses.

##### 2. Pulse-shape measurements

In the experiments on Nd:YAG amplification, the source of input ultrashort pulses for the amplifying rod was a mode-locked low-temperature Nd:YAG laser.<sup>28</sup> The length of the ultrashort pulses was about 80 ps, the maximum energy was 1 mJ, and the beam diameter was 2 mm. A stop that removed peripheral portions of the beam was often placed at the input to the amplifier. This did not have an appreciable effect on the result.

We investigated the pulse shape at exit from the amplifier as a function of the input pulse area  $\theta_0$  (Ref. 10). The area

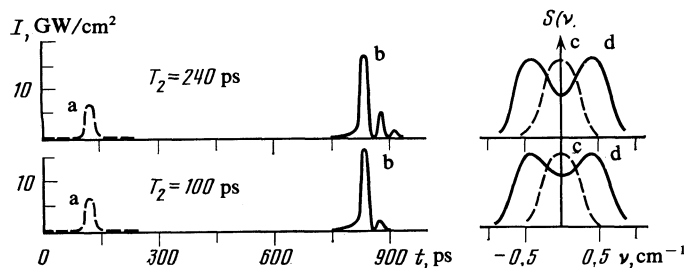


FIG. 5. Coherent amplification in ruby: a and b—input and output pulses, c and d—spectra of input and output pulses;  $L = 12$  cm,  $\alpha L = 6$ ,  $T_2^* = 20$  ps,  $\theta_0 = 0.5\pi$ .

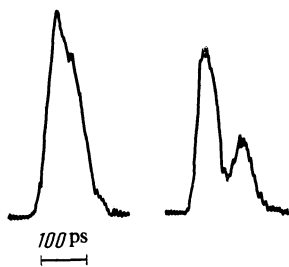


FIG. 6. Densitometer traces of pulses at entrance to (left) and exit from (right) the Nd:YAG amplifier for  $\theta_0 = 0.5\pi$ . The input and output pulse energies are 1 and 5 mJ, respectively.

$\theta_0$  was varied by attenuating the input beam in neutral light filters. For  $\theta_0 \sim 0.5\pi$  and maximum amplification  $\alpha L \sim 5$ , oscillations were observed on the trailing edge of the output pulse (see Fig. 6). When  $\theta_0$  was reduced, the oscillations became less noticeable and the pulse shapes at entry and exit were found to be identical for  $\theta_0 < 0.2\pi$ . The effect was also found to disappear when the temperature of the rod was increased for any achievable value of  $\theta_0$ . For the maximum energy of the input pulse, and also after a double pass through the amplifier, a third burst of low amplitude was often found on the trailing edge. The scale of the time structure was of the order of the Rabi frequency for the pulse field.

To increase  $\theta_0$ , we attempted to produce preliminary amplification of the signal in a 300-mm glass rod containing neodymium. The radiation intensity at entry to the Nd:YAG amplifier was then found to be higher by an order of magnitude as compared with the previous arrangement and, consequently,  $\theta_0$  could reach  $1.5\pi$ , whilst the shape of the ultrashort pulse remained unaltered to within the time resolution of the equipment. However, we did not observe any effects associated with the modulation of the envelope after further amplification in Nd:YAG in the input area range between  $0.1\pi$  and  $1.5\pi$ . The absence of this effect for such high input intensities can be explained by phase (frequency) modulation that may arise during amplification in the Nd glass.<sup>29,30</sup> There is no published information at present on the theory of coherent amplification of phase-modulated pulses. The nearest we have been able to find to a theoretical analysis is given in Ref. 31, but only for conditions quite dissimilar from those obtaining in our experiment.

It is shown in Ref. 32 that a pulse with a modulated envelope can appear as a result of self-focusing in the amplifier. The absence of modulation after preliminary amplification, and the increase in intensity by an order of magnitude, enable us to conclude that under our conditions modulation was unrelated to this effect. Numerical estimates also confirm that self-focusing had little effect.

The change in the shape of the ultrashort pulses that is characteristic for coherent amplification was also occasionally observed in the mode-locked Nd:YAG master oscillator. However, it was more clearly defined during the generation of the ultrashort pulses in ruby at 100 K. The ruby laser was operated under mode-locked conditions. We used a telescopic unstable resonator formed by a 100%-reflecting mirror and a concave glass substrate of radius of curvature equal to 4 m, which acted as the output mirror.<sup>33</sup> The contact

cell with saturable filter consisted of a planar concave lens, whose flat surface was placed against the plane reflecting mirror, with a spacer between them. The entire setup was equivalent to a convex mirror with a radius of curvature equal to 2 m. The filter was a solution of DDI in dimethylsulfoxide. The high ruby transition cross section at 100 K enabled us to produce single-pass amplification of  $\alpha L \sim 6$ . This enabled us to work with a filter with an initial transmission of 2–3%. The properties of mode locking under these conditions are described in our earlier papers.<sup>33,34</sup>

The train of pulses consisted of 2–3 ultrashort pulses with a total energy of 150–200 mJ and 50–100 mJ carried by the largest pulse. The characteristic length of the ultrashort pulses was 40–50 ps and the beam diameter in the active rod was 4–6 mm. The largest pulse in this cavity could be looked upon as the result of amplification after a double pass through the cavity. Figure 7 shows the densitometer tracing for the largest pulse in the train. The trailing edge of the pulse clearly shows the presence of oscillations. As in the case of Nd:YAG, the temporal structure corresponds approximately to the Rabi frequency for the pulse field. For comparison, we also show the densitometer tracing corresponding to the active medium at 190 K. There are no oscillations in this case, whereas, at 100 K, they appeared for practically every laser shot.

From the data on the shape of the envelope at different temperatures, we may conclude that the absence or presence of oscillations on the trailing edge of the ultrashort pulse is determined by the ratio of the characteristic time scale of the pulse to  $T_2$ . This is confirmed by an investigation of the evolution of the pulse shape along the train of ultrashort pulses. Densitometer traces for successive pulses in the train are shown in Fig. 8. The first pulse has no substructure. The subsequent development can be generally described as follows. When the pulse passes through the amplifying medium and the saturable filter, it is effectively reduced in length, as is usual in a two-component medium.<sup>35</sup> When the pulse length becomes less than  $T_2$ , effects associated with the development of coherent polarization in the medium begin to

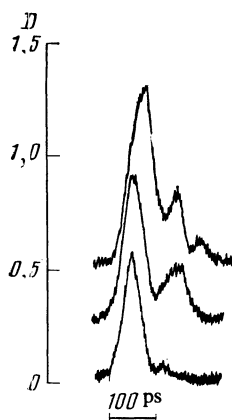


FIG. 7. Densitometer traces of radiation from the self-mode-locked ruby laser. Left—temperature of the medium 100 K; the curves correspond to three successive steps of the attenuator mounted in front of the slit of the electrooptic camera. The temperature of the medium for the right-hand tracing was 190 K. D—photographic density.

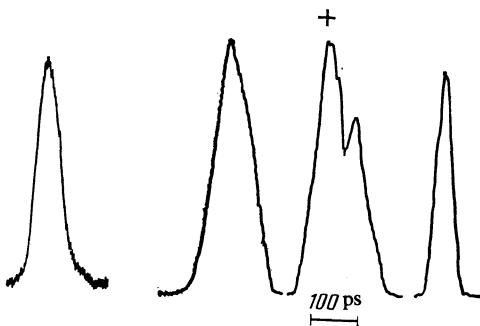


FIG. 8. Evolution of ultrashort pulse along a train in a ruby laser. The cross shows the maximum pulse. The vertical scale is arbitrary for all three pulses.

appear. The trailing edge of the pulse exhibits oscillations which, for the train shown in Fig. 8, can be seen on the largest pulse. The structure of the next pulse is not resolved by the electrooptic camera. This probably corresponds to the contraction of the pulse during its coherent amplification, as should be the case for the self-similar solution of (4) (Refs. 17 and 21). This is confirmed by data on the emission spectrum and on the pulse length, obtained with the aid of a high-speed optical shutter.<sup>34</sup> We note that the variation in the ultrashort pulses along the pulse train is opposite to that recorded for neodymium glass lasers.<sup>29,35</sup> The latter show a substantial broadening of the ultrashort pulses along the train, which is due to nonresonant nonlinearities.

We have also measured the velocity of the pulse during coherent amplification in ruby. We measured the difference between the interval between two successive pulses near the train maximum and the axial period of the resonator. This was done with a calibrated optical delay line consisting of two dense spherical mirrors. The measurement uncertainty was  $\pm 20$  ps. The characteristic "acceleration" of the ultrashort pulses in ruby, as compared with the phase velocity of light, was 10%. In some cases, this figure rose to 30%. This variation in velocity can be explained by its high sensitivity to the shape of the leading edge of the ultrashort pulse.

### 3. Spectral and phase measurements

To determine directly the change in the sign of the field envelope, we investigated the evolution of the phase of the field along the pulse. This was done by time scanning of interference patterns. Interference was produced between light beams reflected from the two surfaces of a plane-parallel glass plate. The far-field interference pattern was then swept across the electrooptic camera. The number of interfering beams in this system was equal to two, and its spectral resolution was very low, but it had very little effect on the shape of the signal and could therefore be used to follow the variation in its phase. Time scans of interference patterns had previously been used in Ref. 36 as a way of exploring phase modulation. The scheme proposed here has the advantage that it is not very sensitive to wave-front aberrations and has a high relative transmission.

The operation of the system is illustrated in Fig. 9, which shows the interference between two pulses with oscillating envelopes when the delay between the pulses corre-

sponds to half the oscillation period. We note that a change in the sign of the envelope can be regarded as a change of  $\pi$  in the phase of the radiation at constant sign of the envelope. When the envelope of the first pulse passes through zero, the phase difference between the interfering pulses changes by  $\pi$ . Constructive interference is then replaced by destructive, and vice versa. A change in the sign of the envelope (or a change of  $\pi$  in the phase) is thus seen as a shift of the interference bands by half the dispersion range of the etalon.

Experiments performed with active elements at 200 K, when  $T_2$  was shorter than the length of the ultrashort pulses under investigation, did not reveal any special phase variation features. The interference bands were found to shift continuously, and this shift corresponded to a quadratic increase in phase, or a linear increase in frequency. The rate of change of frequency was not the same for different bursts, which was probably explained by the dependence of the accumulated phase distortion on the history of the ultrashort pulses in the resonator. Typical values of the rate of change of frequency were  $0.002$ – $0.005$   $\text{cm}^{-1}/\text{ps}$ . It is interesting that the rates of variation of frequency in ruby and in Nd:YAG were roughly the same even though there were considerable differences between intensity levels, and different dyes were employed. The overall change in the frequency of the emission may have been limited by the amplification linewidth of the active medium ( $\sim 1$   $\text{cm}^{-1}$ ).

When the temperature of the active element was reduced to 100 K and coherent amplification was employed, scans of the interferograms revealed in each case the presence of discontinuities and breaks on the interference fringes. Fringe shifts equal to half the dispersion range, which corresponded precisely to the above ideal picture of a phase change of  $\pi$ , were frequently observed. Figure 9c shows an example of this type of scan. Pulse traces recorded

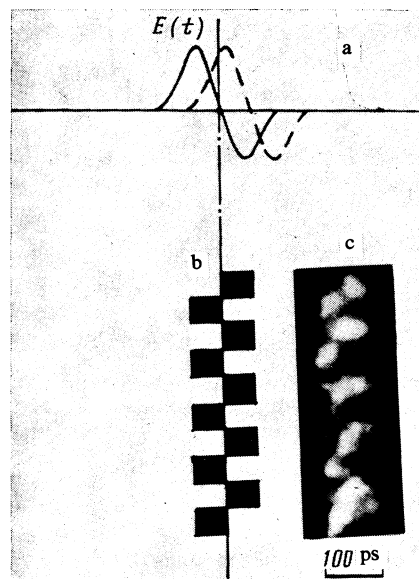


FIG. 9. Interferograms of pulses with oscillating envelopes: a—superposition of pulses (schematic), b—position of interference bands (schematic), c—time scan of interference pattern recorded for the pulse from the ruby laser.

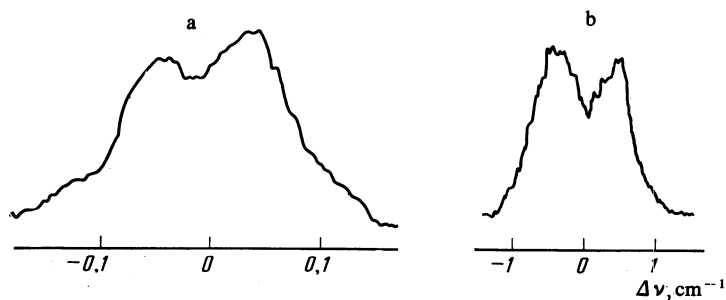


FIG. 10. Densitometer tracings of the spectra of ultrashort pulses at exit from Nd:YAG (a) and ruby (b) amplifiers.

simultaneously with these fringes were always found to show evidence of envelope modulation. These effects occurred both in ruby and Nd:YAG.

The interferograms frequently had a more complicated structure than that indicated in Fig. 9c although they could always be interpreted qualitatively by taking into account the mismatch between the etalon base and the structure of the pulse, the inadequate dynamic range of the equipment, and so on. The above features of phase evolution were recorded even when the equipment did not record the corresponding features on the time profile of the pulse.

The above phase and amplitude properties were found to be reflected in the spectrum of the ultrashort pulses. Densitometer traces of the spectra of pulses amplified in Nd:YAG and ruby rods (Fig. 10) clearly show the doublet structure. The separation between the structure components was consistent with the field oscillation. Because of the limited resolution of the electrooptic camera, the pulse shape in the case of ruby was examined only for the pulse generator. It is interesting that the splitting in the spectrum can be used to estimate the amplitude of the pulse field and, consequently, the intensity of the radiation. The estimated intensity was found to be in good agreement with values calculated from the energy and length of the pulse.

As noted above, ruby differs from Nd:YAG in that the nature of the interaction between radiation and the medium is complicated by the splitting of the ground state of  $\text{Cr}^{3+} (^4A_2)$ , which is equal to  $0.38 \text{ cm}^{-1}$ . The effect of this splitting can be at a maximum during the initial stage of amplification, when the Rabi frequency is less than or of the order of  $0.38 \text{ cm}^{-1}$ . Comparison of the spectra recorded under free-generation and self-mode-locking conditions shows that generation is initially due to the stronger and shorter-wavelength component of the laser transition. The broadening of the spectrum subsequently takes place in an asymmetric manner. Its center of gravity shifts toward the weaker component, whose presence is reflected in the emission spectrum. Thus, the presence of splitting may facilitate the evolution of the doublet structure. However, it is not the dominant effect. This is confirmed by the presence of the doublet structure in the case of amplification in Nd:YAG, for which there is no level splitting, and by measurements of the spectrum of ultrashort pulses amplified in the ruby rod (Fig. 10b). The separation between the components of the doublet may reach about  $1 \text{ cm}^{-1}$ , which is much greater than the ground-state splitting. The corresponding Rabi half-period is about 15 ps, which is outside the range of resolution of our electrooptic camera.

We have recorded pulses of length not greater than 30 ps, which is close to the limit for the measured width of the spectrum. With further amplification, it is possible to produce pulses of length less than the reciprocal of the emission linewidth. This is confirmed by our measurements with a high-speed optical shutter. We found that, when ultrashort pulses from the ruby oscillator at 100 K were amplified by three rods of 120 mm each, we were able to record pulses of 5–10 ps in length, and the spectrum broadened to  $2.0\text{--}2.5 \text{ cm}^{-1}$  (Ref. 34). The fact that ultrashort pulses of length less than the reciprocal of the linewidth can be emitted is due to the broadening of the line in the field of the amplified pulse.

## §5. DISCUSSION

Our investigation of the coherent amplification of ultrashort pulses in Nd:YAG and ruby, using different complementary experimental procedures and a theoretical analysis, has thus yielded detailed information on the evolution of the field and the parameters of the medium. In particular, comparison of experimental data with theoretical calculations enabled us to estimate the transverse relaxation time  $T_2$ . For example,  $T_2 \sim 150 \text{ ps}$  in ruby at 100 K and  $\lesssim 60 \text{ ps}$  at 190 K. The phase change of  $\pi$  indicates the formation of an ultrashort  $0\pi$ -pulse (Ref. 1). The doublet splitting of the spectrum of the amplified pulse, which is due to the dynamic Stark effect, was predicted theoretically and confirmed experimentally. This enabled us to estimate the intensity of the radiation from its spectrum.

Our numerical calculations illustrate the connection between coherent amplification and superradiance.<sup>37</sup> Actually, coherent amplification, like superradiance, is part of the general problem of the evolution of inverted systems in the absence of phase relaxation for different initial conditions for the electric field and polarization of the medium. The quantitative deviation from the self-similar solution that we have found is due to the relatively large length of the input pulse. In this connection, it is interesting to examine the possibility of producing a self-similar pulse during the excitation of uniform polarization by a pulse of length of the order of the superradiance time  $\tau_R$ . The latter time was about 3 ps for both Nd:YAG and ruby under the conditions of our experiment.

From the practical point of view, the attraction of coherent amplification is that it may be possible to use this phenomenon to generate powerful ultrashort pulses. We have developed a compact source of ultrashort pulses incorporating a ruby rod at 100 K, which has been successfully used in studies of laser plasmas.<sup>38,39</sup>

The authors are indebted to M. D. Galanin for his interest and attention, and to A. V. Larikov, R. G. Mirzoyan, and I. R. Sataev for assistance in performing these experiments.

- <sup>1</sup>A. Allen and J. H. Eberly, *Optical Resonance and Two-Level Atoms*, Wiley, 1975 [Russian translation, Mir, Moscow, 1978].
- <sup>2</sup>F. A. Hopf and M. Q. Scully, *Phys. Rev.* **179**, 339 (1969).
- <sup>3</sup>A. Iosevich and W. E. Lamb Jr, *Phys. Rev.* **185**, 517 (1969).
- <sup>4</sup>P. G. Kryukov and V. S. Letokhov, *Usp. Fiz. Nauk* **99**, 169 (1969) [*Sov. Phys. Usp.* **12**, 641 (1970)].
- <sup>5</sup>A. I. Odintsov and V. R. Yakunin, *Pis'ma Zh. Eksp. Teor. Fiz.* **20**, 233 (1974) [*JETP Lett.* **20**, 102 (1974)].
- <sup>6</sup>V. Yu. Baranov, V. L. Berzenko, D. D. Malyuta, *et al.*, *Pis'ma Zh. Eksp. Teor. Fiz.* **30**, 593 (1979) [*JETP Lett.* **30**, 558 (1979)].
- <sup>7</sup>H. K. Chung, J. B. Lee, and T. A. De Temple, *Opt. Commun.* **39**, 105 (1981).
- <sup>8</sup>G. A. Mourou and T. Sizer, *Opt. Commun.* **41**, 47 (1982).
- <sup>9</sup>O. P. Varnavskii, A. N. Kirkin, A. M. Leontovich, *et al.*, *Pis'ma Zh. Eksp. Teor. Fiz.* **37**, 229 (1983) [*JETP Lett.* **37**, 271 (1983)].
- <sup>10</sup>O. P. Varnavsky, A. N. Kirkin, A. M. Leontovich, *et al.*, *Opt. Commun.* **46**, 131 (1983).
- <sup>11</sup>A. M. Leontovich and A. M. Mozharovskii, *Pis'ma Zh. Eksp. Teor. Fiz.* **20**, 664 (1974) [*JETP Lett.* **20**, 305 (1974)].
- <sup>12</sup>O. P. Varnavskii, A. V. Larikov, and A. M. Leontovich, Preprint FIAN SSSR No. 112, 1981.
- <sup>13</sup>A. M. Leontovich and A. M. Mozharovskii, *Pis'ma Zh. Eksp. Teor. Fiz.* **19**, 347 (1974) [*JETP Lett.* **19**, 195 (1974)].
- <sup>14</sup>F. Bloch, *Phys. Rev.* **70**, 460 (1946).
- <sup>15</sup>W. E. Lamb Jr, *Phys. Rev.* **134**, 1429 (1964).
- <sup>16</sup>S. L. McCall and E. L. Hahn, *Phys. Rev.* **189**, 457 (1969).
- <sup>17</sup>D. C. Burnham and R. Y. Chiao, *Phys. Rev.* **189**, 667 (1969).
- <sup>18</sup>G. L. Lamb Jr, *Phys. Lett. A* **29**, 507 (1969).
- <sup>19</sup>V. E. Zakharov, *Pis'ma Zh. Eksp. Teor. Fiz.* **32**, 603 (1980) [*JETP Lett.* **32**, 589 (1980)].
- <sup>20</sup>R. F. Malikov, V. A. Malyshev, and E. D. Trifonov, *Opt. Spektrosk.* **51**, 460 (1981).
- <sup>21</sup>S. V. Manakov, *Zh. Eksp. Teor. Fiz.* **83**, 68 (1982) [*Sov. Phys. JETP* **56**, 37 (1982)].
- <sup>22</sup>D. E. McCumber and M. D. Sturge, *J. Appl. Phys.* **34**, 1682 (1963).
- <sup>23</sup>D. F. Nelson and M. D. Sturge, *Phys. Rev. A* **137**, 1117 (1963).
- <sup>24</sup>T. Kushida, *Phys. Rev.* **185**, 500 (1969).
- <sup>25</sup>J. C. McGillivray and M. S. Feld, *Phys. Rev. A* **14**, 1169 (1976).
- <sup>26</sup>E. D. Trifonov, A. I. Zaitsev, and R. F. Malikov, *Zh. Eksp. Teor. Fiz.* **76**, 65 (1979) [*Sov. Phys. JETP* **49**, 33 (1979)].
- <sup>27</sup>A. M. Leontovich and A. M. Mozharovskii, *Tr. Fiz. Inst. Akad. Nauk SSSR* **98**, 3 (1977).
- <sup>28</sup>O. P. Varnavskii, A. V. Larikov, and A. M. Leontovich, *Kvantovaya Elektron. (Moscow)* **6**, 2452 (1979) [*Sov. J. Quantum Electron.* **9**, 1448 (1979)].
- <sup>29</sup>W. Zinth, A. Lauberau, and W. Kaiser, *Opt. Commun.* **22**, 161 (1977).
- <sup>30</sup>V. V. Korobkin, A. A. Malyutin, and A. M. Prokhorov, *Pis'ma Zh. Eksp. Teor. Fiz.* **12**, 216 (1970) [*JETP Lett.* **12**, 150 (1970)].
- <sup>31</sup>J. A. Armstrong and E. Courtens, *IEEE J. Quantum Electron.* **QE-5**, 249 (1969).
- <sup>32</sup>A. N. Zherikhin, P. G. Kryukov, Yu. A. Matveets, and S. V. Chekalin, *Kvantovaya Elektron. (Moscow)* **1**, 956 (1974) [*Sov. J. Quantum Electron.* **4**, 525 (1974)].
- <sup>33</sup>O. R. Varnavsky, A. N. Kirkin, A. M. Leontovich, *et al.*, *Opt. Commun.* **45**, 342 (1983).
- <sup>34</sup>A. N. Kirkin, A. M. Leontovich, and A. M. Mozharovskii, *Kvantovaya Elektron. (Moscow)* **5**, 2640 (1978) [*Sov. J. Quantum Electron.* **8**, 1489 (1978)].
- <sup>35</sup>N. G. Basov, P. G. Kryukov, V. S. Letokhov, and Yu. A. Matveets, *Zh. Eksp. Teor. Fiz.* **56**, 1546 (1969) [*Sov. Phys. JETP* **29**, 830 (1969)].
- <sup>36</sup>M. Novaro and C. Sauteret, *Opt. Commun.* **32**, 1 (1980).
- <sup>37</sup>R. H. Dicke, *Phys. Rev.* **93**, 99 (1954).
- <sup>38</sup>V. V. Blazhenkov, A. N. Kirkin, A. M. Leontovich, *et al.*, *Zh. Eksp. Teor. Fiz.* **78**, 1386 (1980) [*Sov. Phys. JETP* **51**, 697 (1980)].
- <sup>39</sup>V. V. Blazhenkov, A. N. Kirkin, A. V. Kononov, *et al.*, *Zh. Eksp. Teor. Fiz.* **80**, 144 (1981) [*Sov. Phys. JETP* **53**, 72 (1981)].

Translated by S. Chomet